




Donor-defined mesenchymal stem cell antimicrobial potency against nontuberculous mycobacterium

Tracey L. Bonfield^{1,2,3}  | Morgan T. Sutton^{1,2,3,4} | David R. Fletcher^{1,2,3} |
 Michael A. Folz^{1,2,3} | Vaishnavi Ragavapuram^{1,2,3} | Rodrigo A. Somoza⁵  |
 Arnold I. Caplan⁵ 

¹Department of Genetics and Genome Sciences, Case Western Reserve University, Cleveland, Ohio

²National Center for Regenerative Medicine, Case Western Reserve University, Cleveland, Ohio

³Department of Pediatrics, Case Western Reserve University, Cleveland, Ohio

⁴St. Jude Children's Research Hospital Graduate School of Biomedical Sciences, Memphis, Tennessee

⁵Department of Biology, Skeletal Research Center, Case Western Reserve University, Cleveland, Ohio

Correspondence

Tracey L. Bonfield, PhD, D(ABMLI), Department of Genetics and Genome Sciences, Case Western Reserve University, Cleveland, OH 44106.

Email: tracey.bonfield@case.edu

Funding information

David and Virginia Baldwin Fund; Cystic Fibrosis Foundation; The Marcus Foundation

Abstract

Chronic nontuberculous mycobacterial infections with *Mycobacterium avium* and *Mycobacterium intracellulare* complicate bronchiectasis, chronic obstructive airway disease, and the health of aging individuals. These insidious intracellular pathogens cause considerable morbidity and eventual mortality in individuals colonized with these bacteria. Current treatment regimens with antibiotic macrolides are both toxic and often inefficient at providing infection resolution. In this article, we demonstrate that human marrow-derived mesenchymal stem cells are antimicrobial and anti-inflammatory in vitro and in the context of an in vivo sustained infection of either *M. avium* and/or *M. intracellulare*.

KEYWORDS

human mesenchymal stem cell donor potency and efficacy, lung disease, nontuberculous mycobacteria

1 | INTRODUCTION

There are over 100 000 people in the United States who suffer from chronic nontuberculous mycobacterial pulmonary infections. The infections are difficult to treat, and they significantly impair the quality of life and survival of patients.¹ Nontuberculous mycobacteria (NTMs) are opportunistic intracellular bacteria that are environmentally ubiquitous, becoming pathogenic in individuals with compromised immune systems, including patients with cystic fibrosis (CF), bronchiectasis, pulmonary alveolar proteinosis, or chronic obstructive pulmonary disease (COPD).² NTM infections are also prevalent in older individuals (aged >60 years at 13.9 cases per 100 000 people); however, the

reasons for this susceptibility remain elusive.¹ Treatment for NTM infections includes a 12-month regimen of a macrolide-based, multidrug cocktail, which is often associated with toxicity³ and a significant relapse rate (12%-58%).

Mycobacterium avium complex (MAC) is a complex of NTM species and is the most common NTM isolate identified in non-CF bronchiectasis, COPD, and aging individuals.⁴ Although the species and relative predominance of the NTM that colonizes patients is different, the main players in MAC are *M. avium* and *Mycobacterium intracellulare*.⁵ MACs, like *M. avium* and *M. intracellulare*, are slow-growing bacteria that have complicated the development of standardized in vitro and in vivo modeling systems that can be used to monitor

This is an open access article under the terms of the Creative Commons Attribution-NonCommercial-NoDerivs License, which permits use and distribution in any medium, provided the original work is properly cited, the use is non-commercial and no modifications or adaptations are made.

© 2021 The Authors. STEM CELLS TRANSLATIONAL MEDICINE published by Wiley Periodicals LLC on behalf of AlphaMed Press.

new anti-NTM therapeutics.⁶ In previous studies, we developed an innovative protocol in which *M. avium* and *M. intracellulare* can be evaluated over the course of 1 week instead of 4 to 6 weeks.⁷ This modeling system is used in this article to evaluate the potential of human mesenchymal stem cells (hMSCs) to treat NTM infections.

hMSCs are dynamic storehouses of antimicrobial activity.⁸ Our studies have shown that hMSCs have antimicrobial, anti-inflammatory, and antifibrotic potential both in vitro and in vivo.⁹⁻¹¹ We have also documented that hMSC treatment results in improved effectiveness of antibiotics, thus decreasing the dose required for eradication of bacteria.¹² The studies in this article use in vitro and in vivo models of chronic NTM infection to evaluate the potential therapeutic use of hMSCs. Using these models, we identified donor-specific hMSC potency against *M. avium* and *M. intracellulare*. These data demonstrate the compelling versatility of hMSCs and the potential use of our models to define the ideal therapeutic regimen to treat chronic NTM infections in vivo. Additionally, our studies define the unique hMSC fingerprint related to the capacity to manage NTM infections evaluating the potential for hMSCs to produce heme oxygenase 1 (HMOX-1), interleukin (IL)-6, and macrophage inflammatory protein 3 α (CCL20), which have the capacity to contribute to nontuberculous mycobacterial infection management.^{4,13-15}

2 | MATERIALS AND METHODS

2.1 | Mice

All procedures involving mice were reviewed and approved by Case Western Reserve University's Institutional Animal Care and Use Committee (IACUC 2014-0093). Studies used C57BL/6J wild-type (WT) mice and the CF mouse model B6.129 *Cftr*^{tm1Kth} Tg(FABPCFTR) 1Jaw/Cwr (gut-corrected delF508) and *Cftr*^{tm1Kth} (complete delF508 knockout), which has a cystic fibrosis-like overactive inflammatory response to infection,¹⁶⁻¹⁸ inefficient in resolving pathogens.^{12,19} The complete delF508 has a severe response to infection with high mortality and requires laxatives to attenuate gut obstruction. These are highly expensive mice and hard to breed. The gut-corrected version of delF508 retains the pulmonary hyperinflammatory response to infection, without the same level of mortality associated with the gut contributions to disease. For the purpose of profiling hMSC potency, we use the sublethal model for many of the studies, which were then followed up with the total delF508 strain. Both mouse strains are congenic over several generations on a C57BL/6J background. Although the CF mouse does not recapitulate many aspects of CF lung pathophysiology, it has become the first-line standardized model to monitor infection resolution and uncontrolled inflammation.²⁰⁻²² Other models, like the airway-specific over-expression of the epithelial Na(+) channel (β ENaC) mouse models, provide alternative pathophysiology testing endpoints such as mucociliary clearance or, like the ferret and pig models, have more complete representation of CF pathophysiology.^{20,22} Our studies

Significance statement

Human mesenchymal stem cells have significant clinical utility in treating scenarios of infection and inflammation. Selection of the mesenchymal stem cell source defines the degree of therapeutic potency and potentially efficacy. The studies outlined in this article define human mesenchymal stem cell potency against intracellular bacterial pathogens that are difficult to treat. Choosing the optimal donor for therapeutic impact may provide better outcomes in clinical trials using mesenchymal stem cells for therapeutic potency against these pathogens.

use the murine CF modeling system because they are the first line of studies to evaluate anti-inflammatory therapeutics in the context of chronic infection as standardized by the Cystic Fibrosis Foundation. The reason the model is versatile is that it aids in determining whether anti-inflammatory therapeutics affect infection exacerbation.^{16,19,23} In this article, the model is used to define hMSC anti-inflammatory and antimicrobial potency, which could be translated to other diseases besides CF that are associated with NTM infections.

2.2 | Bone marrow-derived macrophage culture

Bone marrow-derived macrophages (BMDMs) were derived from WT and CF mice as previously described.^{9,24,25} Briefly, hematopoietic cells from the bone marrow were rinsed with 1 \times phosphate buffered saline and centrifuged at 1800 rpm for 9 minutes. After the supernatant was discarded, cells were resuspended with medium (Roswell Park Memorial Institute medium (RPMI) + 10% heat inactivated fetal bovine serum (HI-FBS) + 1% penicillin-streptomycin (PSG) + 46mL L929 generated conditioned medium) and plated at 2.5×10^6 cells in 5 mL per petri dish.

2.3 | NTM culture conditions

M. avium (#49601; American Type Culture Collection, Manassas, Virginia) and/or *M. intracellulare* (#13950; American Type Culture Collection) were suspended using 7H9 broth. From the resuspended bacteria, 1 mL was used to grow bacterial culture in a 125-mL Erlenmeyer flask with 12 mL broth (7H9 broth, #M0178-500 g; albumin-dextrose-catalase (ADC) enrichment, #M0553-1 VL; Sigma, St. Louis, Missouri) and was incubated at 37°C with 5% CO₂.⁷ Culture medium was changed every 5 days with 10 mL fresh 7H9 broth to continue growth. Optical density was monitored at every collection and medium change to ensure proper pathogenic concentration. *M. avium* complex and the participating NTM pathogens are highly variable depending on the isolate. *M. avium* and *M. intracellulare* are generally the dominant species.

The model used to mimic *Mycobacterium avium* complex (MAC) consisted of 50% *M. avium* and 10% *M. intracellulare*.

2.4 | In vivo models of NTMs

M. avium and *M. intracellulare* were cultured 1 week by adding 1 mL of bacterial stock to 12 mL of Middlebrook 7H9 broth as extensively described previously.^{16,26} One week later, bacterial optical density was measured (600 nm) to define the concentration of either NTM pathogen to put directly into mice (acute infection/inflammation model) or into the bead preparation (sustained infection model) defined by the optical density/colony forming unit (CFU) relation of either *M. avium* or *M. intracellulare*.⁷ All mice had spleen, liver, and lung CFU quantification.

2.5 | Acute infection

Mice were anesthetized with isoflurane followed by instilling, through the intranasal passageway, 100 μ L of 10⁶ CFUs of NTMs.

2.6 | Sustained infection

NTMs were embedded into agarose beads as previously described.¹⁶ The NTM bead preparations were diluted 1:50, 1:500, 1:5000, and 1:50 000 and plated on 7H9 agar plates (M9029; Teknova, Hollister, California) to validate the dosing/bead preparation prior to use in vivo. Agarose beads were prepared and verified for CFUs to verify NTM dosing.^{12,19,27} Once the CFUs for the pathogen bead preparations were known, beads were diluted so that each animal received 10⁵ CFUs in 50 μ L using transtracheal infusion. After surgery, the diluted solution was plated once more on 7H9 plates and incubated overnight to validate infection with dosing the mice. Mice were monitored each day up to day 7 by tracking individual weights and thermal imaging for clinical score. Serum and bronchoalveolar fluid were obtained at termination for monitoring inflammation and infection status. Mouse models are notoriously excellent at resolving pulmonary infections, which is why the agarose bead model is used to establish a long-term infection.^{28,29} The beads themselves degrade over time, which is essential because foreign bodies in the lung create granulomas and foreign body reactions.^{30,31} Free bacteria are resolved within 24 to 48 hours, so the use of the agarose bead model allows for extension of the infection and transition of the inflammatory response. In this article, the 7-day NTM model is used to establish hMSC potency in vivo.

2.7 | Thermal imaging

Individual mice were placed in a polyvinyl chloride (PVC) ring roughly 4.5 inches tall, on a nonreflective surface kept at constant temperature. An infrared camera (FLIR, Wilsonville, Oregon) was held above the ring at a standard height, and a picture was taken. Photos were then analyzed by

converting to a series of temperature measurements at specified locations on the body of the mouse using FLIR Tools software. Measuring a series of external temperatures of the mouse allows for an estimate of internal temperature, which in turn provides a clinical score to describe overall inflammation and overall health. The clinical score ranges from 0 to 12, with a higher score suggesting better survivability and lower overall inflammation. A score of 4 or below is indicative of poor infection resolution and a decreased probability of next-day survivability. These clinical scores are comparable to other observable metrics of health such as weight and postmortem bacterial load. The thermal imaging was used to evaluate the acute response to infection out to 3 days and the sustained response out to 7 days as verified by CFUs and weight changes.

2.8 | Human mesenchymal stem cells

Human posterior iliac crest bone marrow samples were obtained after written informed consent with Case Western Reserve University and University Hospitals Internal Review Board (#CASE12Z05). hMSCs were isolated and expanded in ex vivo culture per previously published methods.³²⁻³⁴ Pre-good manufacturing practices (GMP) procedures have also been previously described.³⁵ hMSCs (passage 2 or 3) were grown in antibiotic-free conditions for 3 days prior to harvesting the conditioned medium (supernatant) or cells for use in these studies. Table 1 details the deidentified hMSC preparations for age range, demographics, and gender that were made available. hMSC antibiotic-enhancing activity involved culturing the hMSCs and gentamicin (10 ng/mL) concurrently with *M. avium*, *M. intracellulare*, or MAC CFUs.

2.9 | Luminex assay

Assays were obtained from R&D Systems (Minneapolis, Minnesota) and done according to the manufacturer's instructions using a Luminex[®] 100/200™ System 0/200 evaluating the following: tumor necrosis factor (TNF)- α , IL-6, IL-1 β , and keratinocytes-derived chemokine (KC). BMDMs (n = 3 different preparations) in duplicate were treated with *M. avium* or *M. intracellulare* either as a free solution or embedded into agarose beads. Cell culture supernatants from each of the BMDM experiments were harvested 24 hours later, aliquoted, and frozen prior to the Luminex assays. The multiplex assay was processed according to the manufacturer's directions using a Five Parameter Logistic (5PL) curve fit.^{36,37} LL-37 was quantified using an enzyme-linked immunosorbent assay as previously described using our Clinical and Translational Science Collaborative (CTSC) Bioanalyte Core, which is directed by Dr Bonfield.^{9,12}

2.10 | Reverse transcription polymerase chain reaction

mRNA extraction was performed through phenol extraction followed by cDNA to monitor gene expression using reverse transcription

TABLE 1 hMSCs donor sources profiled for anti-NTM studies

Donor	Gender	Age (years)
A	Female	40-50
B	Male	30-40
C	Female	20-30
D	Not provided	Not provided
E	Not provided	Not provided
F	Male	20-30
G	Not provided	Not provided
H	Not provided	Not provided
I	Not provided	Not provided
J	Female	30-40
K	Male	30-40
L	Female	40-50
M	Male	30-40
N	Male	30-40
O	Male	40-50
P	Male	20-30
Q	Male	20-20
R	Male	30-40

polymerase chain reaction. Quality of mRNA and cDNA was assessed through NanoDrop spectrophotometry (optimal threshold 260-280 nm; Thermo Fisher Scientific, Waltham, Massachusetts).^{9,11,37} Validation of cDNA quality was done through use of a reference gene peptidyl prolyl isomerase (hPPIA; Hs04194521_s1). Validated primers were obtained from Applied Biosystems (Foster City, California) for IL-6 (Hs00174131_m1), HMOX-1 (Hs01110250_m1), and CCL20 (Hs00355476_m1), which were normalized to the validated internal expression of hPPIA. Data is expressed as fold change of IL-6, HMOX-1, CCL20 gene threshold cycle value as compared to the housekeeping hPPIA gene.

2.11 | Statistical analysis

Analyses of linear or log transformation were used to compare between experimental conditions using unpaired *t* tests, and one-way analysis of variance (ANOVA) quantified assays also used comparisons of slopes over time.^{38,39} In the acute and chronic infection models, survival curves were compared using stratified log-rank tests with pathogens *M. avium* and *M. intracellulare* as strata. When comparing cytokine levels, paired *t* tests were used, assuming that SDs of 0.75 on the log₂ scale by a 2.8-fold differences in expression can be detected with 80% power with two-sided tests at the .01 significance level.⁴⁰ Pathology (eg, bacterial load, white blood cell counts, and cytokines) was log-transformed as necessary to compare between groups or conditions using one- or two-way ANOVA, treating donors as experimental blocks. Prism software (version 9.0.2; GraphPad Software, La Jolla, California) was used for analyses.

One-way ANOVA and Bartlett's correction were incorporated to manage multiple variables and correction for data normalization when required. All significance was defined by the 95% confidence interval at $P \leq .05$.

3 | RESULTS

3.1 | hMSC anti-NTM potency

We have previously described a systematic way to follow the growth, metabolism, and survival of *M. avium* and *M. intracellulare*.⁷ We have also described the potential for hMSCs and their secreted products to have antimicrobial and anti-inflammatory potential.⁹⁻¹¹ Given these findings, we focused on the potential of hMSCs for anti-nontuberculous mycobacterial activity. To begin these studies, we first performed in vitro assays to determine whether hMSCs and their secreted products had anti-nontuberculous mycobacterial potential and whether the supernatants and cells had differential effects on the nontuberculous mycobacteria (Figure 1). We found the hMSCs and their supernatants to have differences in their ability to affect MAC (Figure 1A), *M. intracellulare* (Figure 1B), and *M. avium* (Figure 1C) CFUs in vitro over 24 hours. hMSCs significantly decreased CFUs in MAC, trended toward significance in *M. intracellulare*, and significantly decreased *M. avium* CFUs. Supernatants decreased CFUs in all conditions but were only significantly effective in MAC (Figure 1A). Given these findings, we wanted to evaluate the effect of the hMSCs on the nontuberculous mycobacteria over a longer time span as well as to assess the impact of different hMSC donor preparations.

Supernatants from 12 different donor preparations of hMSCs were cultured with MAC, *M. intracellulare*, and *M. avium*. Figure 2A focuses on how each of the hMSC supernatant preparations affects the survival of MAC from 24, 48, and 72 hours of treatment as defined by CFUs compared with MAC without hMSC treatment (culture medium control). This panel demonstrates the percent decreased number of CFUs of each preparation of MAC without and with hMSC supernatant treatment. Each color represents a different hMSC donor preparation. The ability to decrease MAC growth was variable by hMSC preparation, with some hMSC supernatants approaching 100% capacity to kill MAC and others showing much lower capacity to kill MAC, across 24, 48, and 72 hours of treatment. With culture conditions were extended to 72 hours, we could evaluate the hMSC preparations for sustained anti-MAC activity, which showed that the sustainability of the anti-NTM effect was also hMSC donor dependent (Figure 2A). These data demonstrate that each of the hMSC donor supernatants exhibits different antimicrobial potency and potential for sustainable efficacy in vitro.

Because MAC is composed of both *M. avium* and *M. intracellulare*, the next series of studies explored how donor hMSC preparations affected each NTM individually, hypothesizing that the variability may be related to hMSC donor-specific NTM-specific antimicrobial activity. To begin to determine if the variability observed in the hMSC anti-MAC potency was due to a specific species of nontuberculous

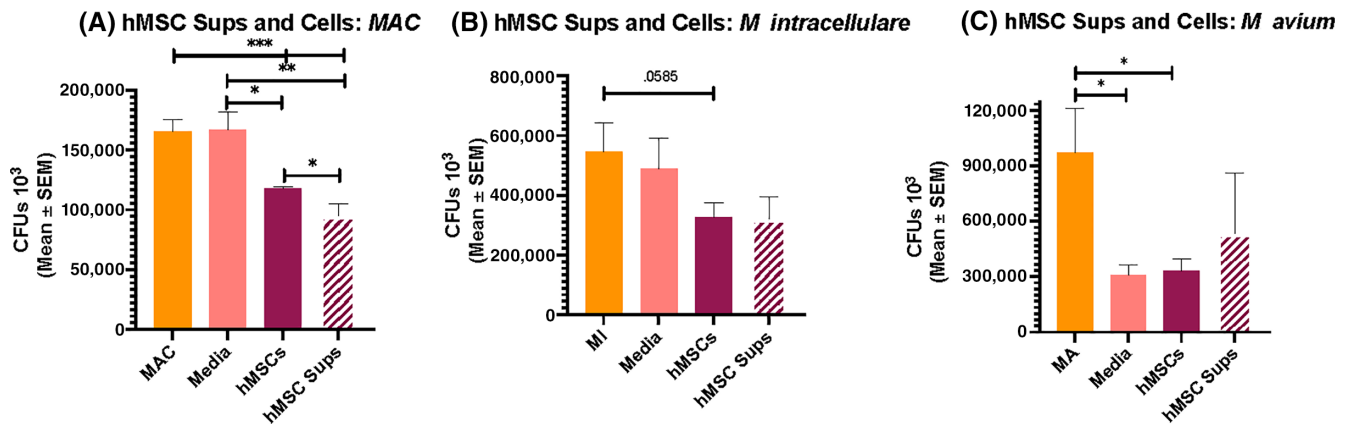


FIGURE 1 hMSC cell and supernatant anti-nontuberculous mycobacterial potency. hMSC growth medium, hMSC cells, or hMSC supernatant (antibiotic-free 72-hour conditioned medium) was cultured with MAC (A), *M. intracellulare* (B), or *M. avium* (C) for 24 hours. Conditions were plated on 7H9 agar plates and evaluated 3 days later. hMSC cells and supernatants significantly decreased MAC CFUs (A; $P < .005$ and $P < .0005$, respectively) and CFUs compared with hMSC growth medium ($P < .05$ and $P < .005$, respectively). There was also a significant difference between hMSC cells and supernatants in the effects on MAC CFUs ($P < .05$). The hMSCs and their supernatants did not have a statistically significant effect on *M. intracellulare* CFUs (B); however, hMSCs trended toward significance ($P = .0585$). In *M. avium*, the hMSCs were the only group to have a statistically significant effect on CFUs (C; $P < .05$). CFU, colony forming unit; hMSC, human mesenchymal stem cell; MA, *M. avium*; MAC, *M. avium* complex; MI, *M. intracellulare*; sup, supernatant. ns = $P > .05$, * $P < .05$, ** $P < .005$, *** $P < .0005$

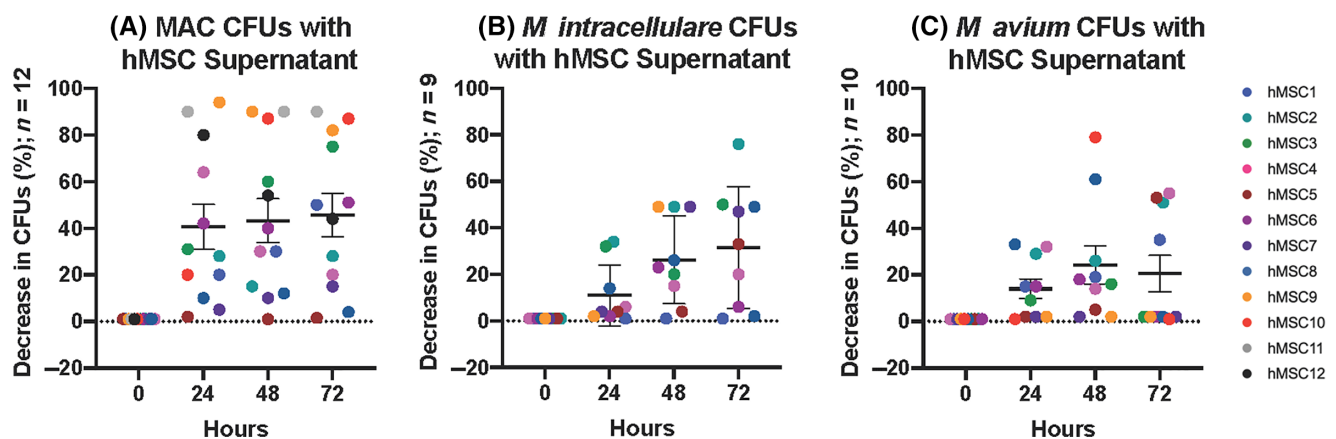


FIGURE 2 hMSC supernatant anti-nontuberculous mycobacterial long-term potency. A, hMSC supernatants from antibiotic-free 72-hour conditioned medium were co-cultured with MAC. Cultures were allowed to proceed for 3 days with a daily evaluation of pathogen burden by CFUs. Bacteria were plated on 7H9 plates and incubated for 3 days to allow for evaluation of the colonies. The majority of the hMSC preparations had anti-MAC activity, but the kinetics of the anti-MAC activity changed over time and were donor dependent. B, hMSC supernatants from antibiotic-free 72-hour conditioned medium were co-cultured with *M. intracellulare*. Cultures were allowed to proceed for 3 days with a daily evaluation of pathogen burden by CFUs. The majority of the hMSC preparations had anti-MI activity, but the kinetics of the anti-MI activity changed over time, and there was large donor variability. C, hMSC supernatants from antibiotic-free 72-hour conditioned medium were co-cultured with *M. avium*. Cultures were allowed to proceed for 3 days with a daily evaluation of pathogen burden by CFUs. The majority of the hMSC preparations had anti-*M. avium* activity with the anti-*M. avium* activity changing with time and hMSC donor preparation. CFU, colony forming unit; hMSC, human mesenchymal stem cell; MAC, *M. avium* complex

mycobacteria, each of the hMSC preparations was screened against *M. intracellulare* (Figure 2B) and *M. avium* (Figure 2C) separately. The results demonstrated that there was significant variability in the ability of the hMSC supernatants to affect *M. intracellulare* or *M. avium* CFUs. Additionally, the kinetics of the different hMSCs donor preparations on *M. intracellulare* (Figure 2B) and *M. avium* (Figure 2C) were substantially variable. The hMSC supernatant donors each had their own profile, suggesting that selection of the hMSC preparation for treatment would

be based upon which pathogen was being treated and whether the application required an immediate or sustained antimicrobial effect. The differences between hMSC supernatant effects on *M. avium* and *M. intracellulare* would likely define anti-MAC potency because *M. avium* is the dominant species in MAC. If a preparation is not efficient against *M. avium* but kills *M. intracellulare*, it may not have the same clinical benefit as an hMSC preparation that is potent against both if a patient is infected with MAC, rather than a singular NTM.

Antimicrobial potency and therapeutic efficacy are also defined by the ability to enhance sensitivity to antibiotics. In previous studies, we have shown that hMSCs and their secreted products have the capacity to enhance antibiotic effects.¹¹ To determine if the hMSC supernatants would affect the sensitivity of the NTMs to antibiotics, we cultured the hMSCs with MAC, *M. avium*, or *M. intracellulare* with and without the addition of gentamicin. Although gentamicin is not a macrolide, it does have anti-NTM potency and provides a good indication for the potential for antibiotic-enhancing potential based upon our previous work.^{11,41} Four of the preparations highlighted in Figure 2 were tested in the presence and absence of suboptimal concentrations of gentamicin (10 ng/mL; Figure 3). There was significant variability in the antibiotic-enhancing potency of each hMSC donor preparation, with two of the hMSC preparations having high antibiotic-enhancing potential approaching 70% to 80% at 72 hours for MAC (Figure 3A). The other two preparations provided action against MAC activity, but the potency was not sustainable. Evaluating the same hMSCs against the individual pathogens *M. intracellulare* and *M. avium* demonstrated the overall capacity to enhance sensitivity to antibiotics. In *M. intracellulare*, there was sustained impact of the hMSC supernatant and gentamicin on CFUs, with 40% to 60% maximum at 72 hours (Figure 3A). The same two preparations that had the highest potency against MAC and *M. intracellulare* (Figure 3; hMSC1 and hMSC2) also had the highest potency against *M. avium* (Figure 3C) approaching 60% to 80% at 72 hours. The antibiotic-enhancing capacity of the two best preparations was much higher in MAC and *M. avium* than in *M. intracellulare*, consistent with the dominance of *M. avium* in MAC.

3.2 | In vivo models of NTM infection

To transition in vitro studies to in vivo models, we used the WT and CF pathogen modeling systems to develop a standardized in vivo

model of NTM infection. We chose to examine *M. intracellulare* and *M. avium* separately for these studies to better understand the impacts of each pathogen before proceeding into dual pathogen in vivo studies. Initially, a 10^6 CFU inoculum of *M. avium* or *M. intracellulare* was administered intranasally into WT and CF mice (Figure 4). WT mice resolved the *M. intracellulare* and *M. avium* infection better than the CF mice, based on CFU bacterial load in the lung (Figure 4A,B). None of the mice had spleen or liver CFUs per our assay of these tissues. However, both WT and CF mice lost weight with the *M. intracellulare* and *M. avium* infection but resolved weight loss at similar rates by day 3, consistent with resolving an infection (Figure 4C,D). To enhance our ability to monitor the infection without euthanizing the mice, we used our thermal imaging technology to monitor the infection response longitudinally in the mice. The thermal imaging technology provides insight into the host response in vivo. The data that are obtained from the thermal image transform the thermal heat map into a quantitative clinical score with minimal stress to the mice.⁴² The imaging profiles of a WT and CF mouse infected with *M. intracellulare* (Figure 4E) or *M. avium* (Figure 4F) are shown. Day 0 is the thermal image of the mice prior to the free *M. intracellulare* or *M. avium* infection along with their weight and thermal score. After infection, the mice were imaged on days 1, 2, and 3 prior to euthanasia. With *M. intracellulare*, the representative WT mouse loses minimal weight on day 1 and regains weight and improves thermal score by day (Figure 4E). The representative CF mouse loses weight and has a decreased thermal score until day 3 (Figure 4E). With *M. avium*, the representative WT mouse stays consistent in both weight and thermal score, whereas the representative CF mouse stays consistent in weight and thermal score early on but loses weight and decreases thermal score on the last 2 days (Figure 4F). These changes in thermal score and weight with *M. intracellulare* and *M. avium* infection were profiled and compared across the experiments to demonstrate the accuracy of the thermal imaging technology in predicting

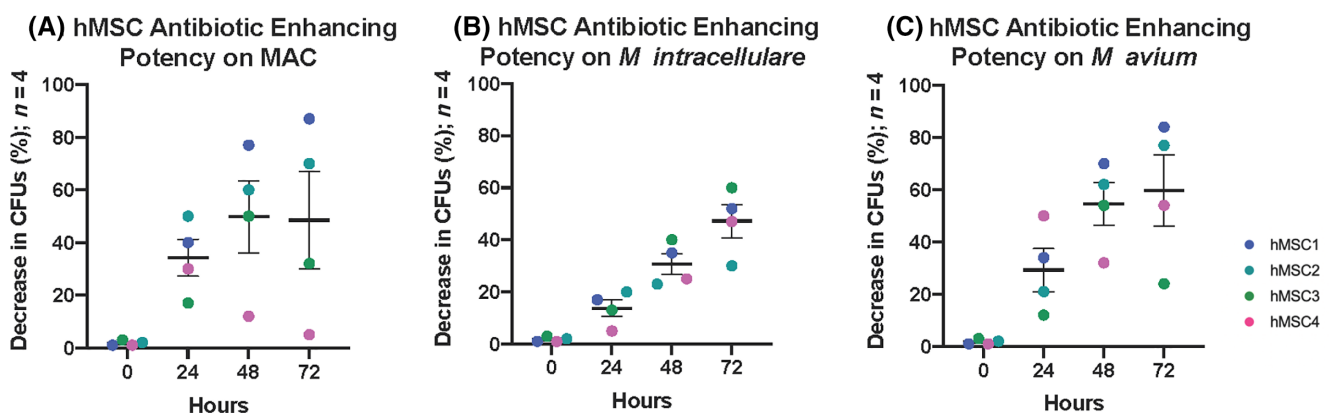


FIGURE 3 hMSC nontuberculous mycobacterial antibiotic-enhancing potency. hMSC supernatants from antibiotic-free 72-hour conditioned medium were co-cultured with MAC (A), *M. intracellulare* (B), or *M. avium* (C) with and without concurrent addition of 50 μ g/mL gentamicin. Cultures were allowed to proceed for 3 days with a daily evaluation of pathogen burden by CFUs. Bacteria were plated on agar plates and incubated for 3 days to allow for evaluation of the colonies. The majority of the hMSC preparations had antibiotic-enhancing potency, but the impact was variable depending on the pathogens evaluated. There was large variability in effectiveness over time between donors. CFU, colony forming unit; hMSC, human mesenchymal stem cell; MAC, *M. avium* complex

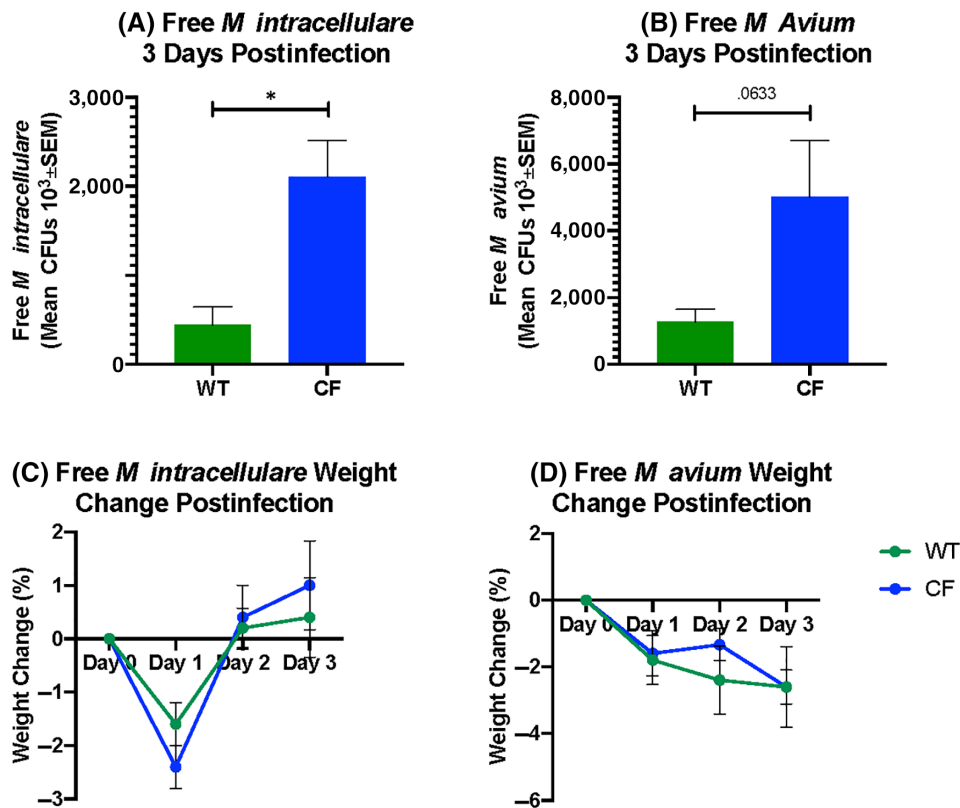


FIGURE 4 Free *M. avium* and *M. intracellulare* in vivo model. WT and CF mice were infected with 10^6 CFUs of free *M. intracellulare* (A), *M. avium* (B), and followed for 3 days for CFUs, weight, and thermal score. A,B, Mean CFUs 3 days after infection for *M. intracellulare* and *M. avium*, respectively, in WT and CF mice. C,D, Percent weight change over the course of the study compared with baseline weight prior to infection for *M. intracellulare* (C) and *M. avium* (D). E-H, Thermal imaging of the mice on each day of the experiment was performed using FLIR camera. Representative thermal images with corresponding weight and thermal score are shown for *M. intracellulare* (E) and *M. avium* (F). Thermal image scores were compared with percent weight change over the course of the study to demonstrate accuracy of thermography scoring system for *M. intracellulare* (G) and *M. avium* (H). CF, cystic fibrosis; CFU, colony forming unit; MA, *M. avium*; MI, *M. intracellulare*; WT, wild type. * $P < .05$

inflammation status and clinical score (Figure 4G,H). The studies emphasize both our efficiency at infecting the mice with the different NTM species in an acute setting of infection and the fact that in the acute setting there is little, albeit some, difference in the infection trajectory between WT and CF mice infected with NTMs. NTM infections do not tend to be acute but consistently transition to more insidious and long-lasting infections in CF.

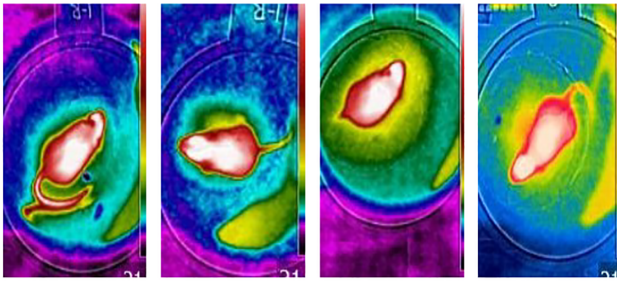
hMSC therapeutic development to treat chronic NTM infections requires a model that can recapitulate a longer infection and inability to effectively resolve the NTM infection, such as that is seen in human disease. To address this need, we adopted our standardized agarose bead infection modeling system, which we use to evaluate antipathogen and anti-inflammatory therapeutics for potency and efficacy to NTM infection.^{9,16,17} For these studies, we embedded *M. intracellulare* and *M. avium* with a known viable inoculum of 10^6 CFU of bacteria (based upon optical density and CFUs) into an agarose/bead-mineral oil matrix of 5 to 10 μm . Pathogens can respond to the modeling matrix differently in terms of sensitivity to heat and manipulation thus verifying that the process of preparing the agarose beads did not alter the growth of the NTMs by culturing the agarose bead preparations embedded with *M. intracellulare* or *M. avium* to evaluate

the survival and pathogenic load of each species (Figure 5A). After assuring the capacity of the pathogens to survive in the modeling technology, we translated the bead count of CFUs/bead numbers to consistently deliver 10^6 CFUs for the in vivo mouse model. The next goal was to determine if the *M. intracellulare* and *M. avium* bead preparations could induce a sustained infection in vivo using the CF and WT mice. Using the validated agarose bead-NTMs preparations in Figure 5A, we infected WT and CF mice with *M. intracellulare* or *M. avium* and followed the mice for 7 days. Both WT and CF had sustained infection at day 7 (Figure 5B,C). The studies demonstrate the ability to generate a more sustained in vivo infection model of *M. intracellulare* and *M. avium* and highlight the differences in the infection trajectory between the WT and the CF mice.

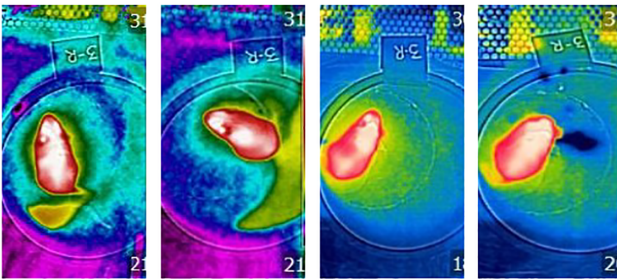
3.3 | Therapeutic efficacy of the different donor hMSCs in vivo

With the establishment of the model, we wanted to test if the donor hMSC potency differences in vitro correlated to in vivo efficacy. Both hMSC cells and the supernatants have anti-NTM activity (Figure 1).

(E)

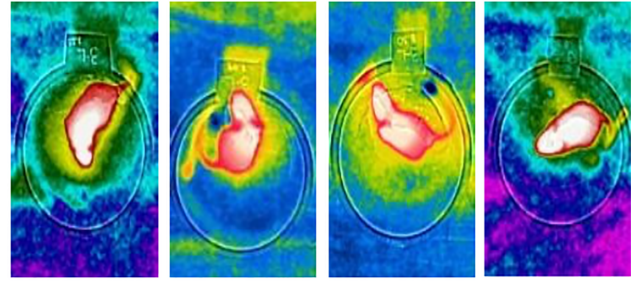


WT- Thermal Score (MI Free)	8	8	9	10
	Day 0	Day 1	Day 2	Day 3
Daily Weight (g)	17.7	17.5	17.9	18.1

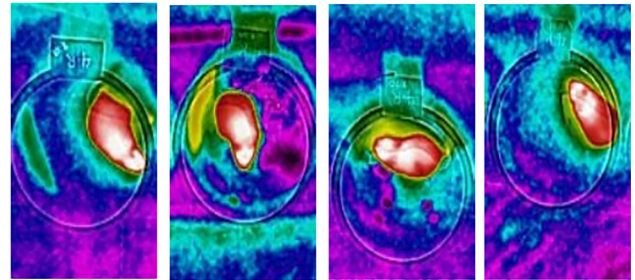


CF- Thermal Score (MI Free)	9	6	7	9
	Day 0	Day 1	Day 2	Day 3
Daily Weight (g)	19.1	18.5	19	19.2

(F)

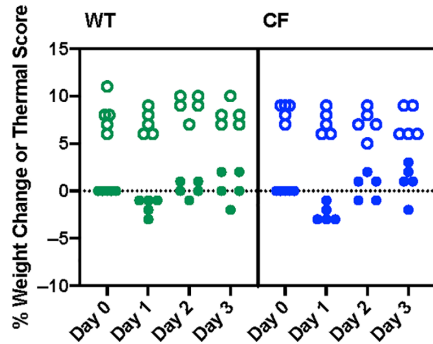


WT- Thermal Score (MA Free)	7	6	7	7
	Day 0	Day 1	Day 2	Day 3
Daily Weight (g)	25.8	26.1	26.1	25.7



CF- Thermal Score (MA Free)	6	7	6	3
	Day 0	Day 1	Day 2	Day 3
Daily Weight (g)	27.1	27.1	26.9	26.3

(G) *M. intracellulare* Weights and Thermal Scores



(H) *M. avium* Weights and Thermal Scores

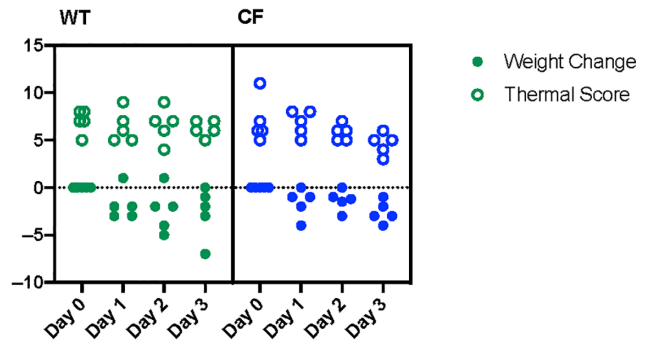


FIGURE 4 (Continued)

hMSCs manage the surrounding milieu through the production of soluble mediators, which is why each of the hMSC donor supernatant preparations was screened against the NTMs (Figure 1). However, the in vivo models receive intact cells and not the supernatants. Based on the results of the beginning studies, the most efficacious hMSC donor ($10^6/100 \mu\text{L}$ given through the retro-orbital sinus) was used to treat WT and CF mice infected 24 hours earlier with agarose beads embedded with 10^5 CFUs of either *M. intracellulare* (Figure 5D) or *M. avium* (Figure 5E). In evaluating the in vivo bead models, the CF mice consistently had higher CFUs relative to the WT mice at day 7 (Figure 5D,E) regardless of the pathogen. None of the mice suffered from NTM

decompartmentalization, quantified by negative spleen, liver, and blood CFUs. The administration of hMSCs in the CF mice resulted in significantly decreased lung CFUs of both *M. intracellulare* and *M. avium* infection compared with CF mice not treated with hMSCs at day 7 (Figure 5D,E). Again, mice had negative spleen, liver, and blood CFUs. In the *M. intracellulare* bead model, all mice had sustained inflammation in response to infection; however, the CF mice had significantly higher lung CFUs at 7 days compared with WT or CF treated with hMSCs (Figure 6A). All *M. intracellulare* bead-infected mice lost weight over the course of the 7 days; however, the hMSC-treated CF mice brought the percent weight change back to that of

the WT (Figure 6B). Thermal imaging was performed on the NTM bead models over the course of the 7 days, starting from the day prior to infection. Figure 6C demonstrates the thermal imaging of representative *M. intracellulare* bead-infected WT, CF, and CF + hMSC mice with correlating thermal score and weight. The representative WT mouse lost weight on day 4 postinfection but regained weight by day 7, which correlated with thermal score (Figure 6D). The representative CF mouse lost significant weight over all 7 days of the infection study and had a similarly decreasing thermal score commensurate with weight loss (Figure 6E). The representative CF mouse given hMSCs lost weight during the first 4 days postinfection and started to regain weight on day 7, which correlated with thermal score on days 0 through 7 (Figure 6F). These studies indicate that hMSCs have the capacity to attenuate the NTM infection course in the CF mice,

attenuating lost weight, thermal score, and pathogenic load. MAC was not pursued in the agarose bead model at this time because the ratio of *M. intracellulare* and *M. avium* is variable between different MAC isolates and the relative sensitivities of *M. intracellulare* and *M. avium* to the different hMSC preparations were different. Future studies are aimed at combining agarose bead preparations so that changes in exact *M. intracellulare* and *M. avium* ratios can be incorporated.

3.4 | Nontuberculous mycobacterial bead preparations and macrophage response

The goal of the agarose bead preparation was to sustain the pathogen in vivo and to provide a potent NTM signal for an immune response.

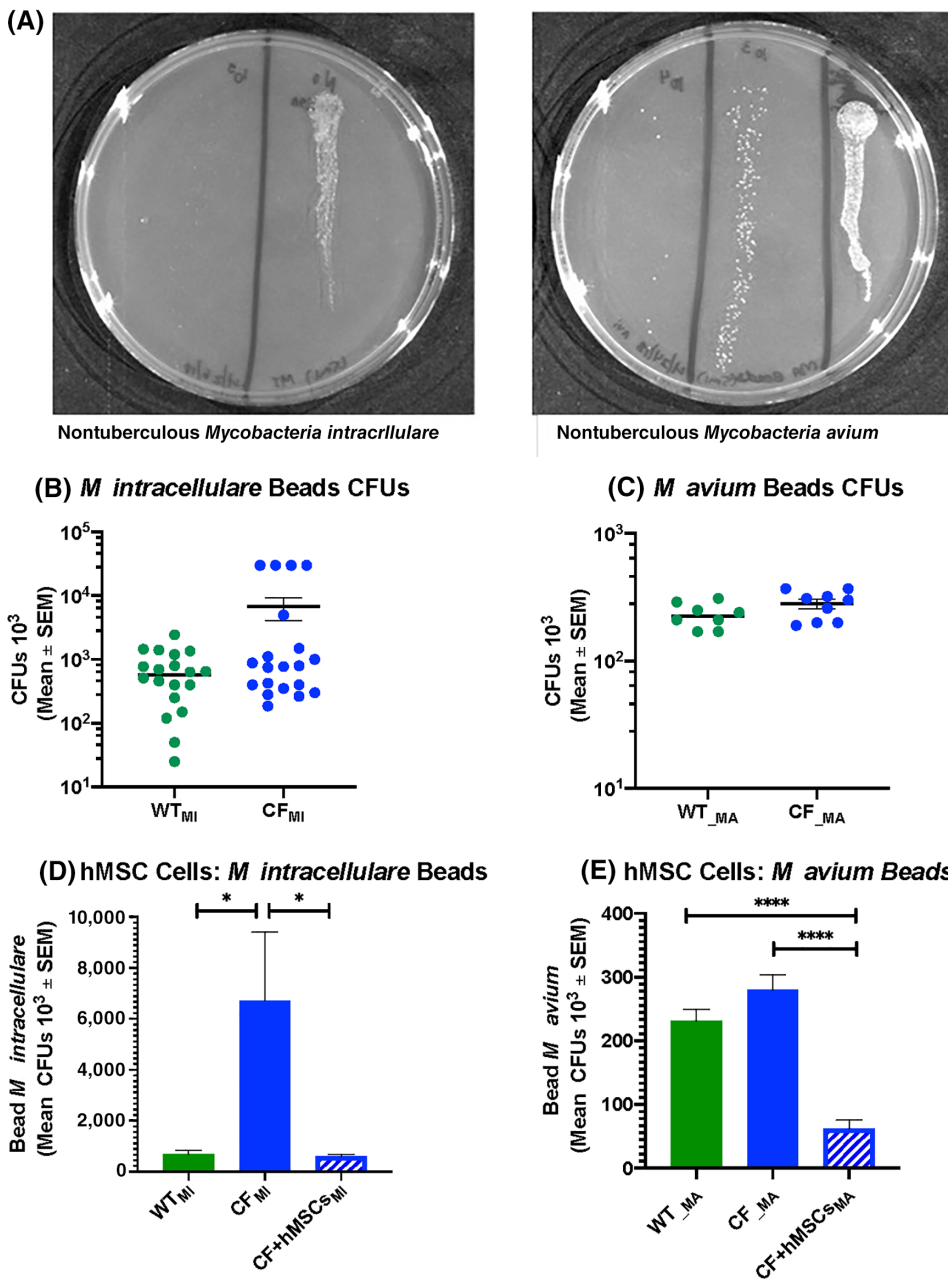


FIGURE 5 Development of the in vivo sustained *M. intracellulare* and *M. avium* infection model. A, Using growth conditions optimized for *M. intracellulare* and *M. avium*, we validated the ability to embed into agarose beads. These beads were tested for potency; results are shown in Table 2. B,C, The same bead preparations were used to infect C57BL/6J or *Cftr*^{tm1Kth} knockout mice. Mice were euthanized, and whole lung homogenate lung CFUs were defined for *M. intracellulare* (n = 20) (B) and *M. avium* (n = 10) (C). D,E, Wild-type (WT) and cystic fibrosis model (CF) mice were infected with *M. intracellulare* (D) or *M. avium* (E) beads, and a group of CF mice was also given hMSC cells retro-orbitally to determine potency of hMSCs on nontuberculous mycobacteria (NTM) infection in vivo, as defined by lung homogenate CFUs. hMSCs significantly decreased *M. intracellulare* CFUs in the CF mice (D; $P < .05$). In the *M. avium* infection model, hMSC significantly decreased CFUs in the CF mice (E; $P < .0001$) and even decreased the CFUs of the CF mice compared with WT ($P \leq .0001$). None of the mice had detectable spleen or blood NTM CFUs. * $P < .05$, **** $P < .0001$, CF_{MA}, CF mice infected with *M. avium* treated; CF_{MI}, CF mice infected with *M. intracellulare*; CF_{MA} + hMSC, CF mice infected with *M. avium* treated with hMSCs; CF_{MI}, CF mice infected with *M. intracellulare* treated with hMSCs; CFU, colony forming unit; hMSC, human mesenchymal stem cell; WT_{MA}, wild type mice infected with *M. avium*; WT_{MI}, wild type mice infected with *M. intracellulare*

Nontuberculous mycobacteria are intracellular pathogens that infect macrophages as the primary site of intrusion. To verify that the process of embedding the NTM into the agarose beads did not alter the signal potency of the pathogens, the agarose bead-NTM preparations

were cultured with BMDMs, with the BMDMs analyzed for the inflammatory response. CF BMDMs are known to have a more robust response than WT BMDMs and have consistently been used to follow changes in immune response in vitro.^{19,43,44} To evaluate the potency

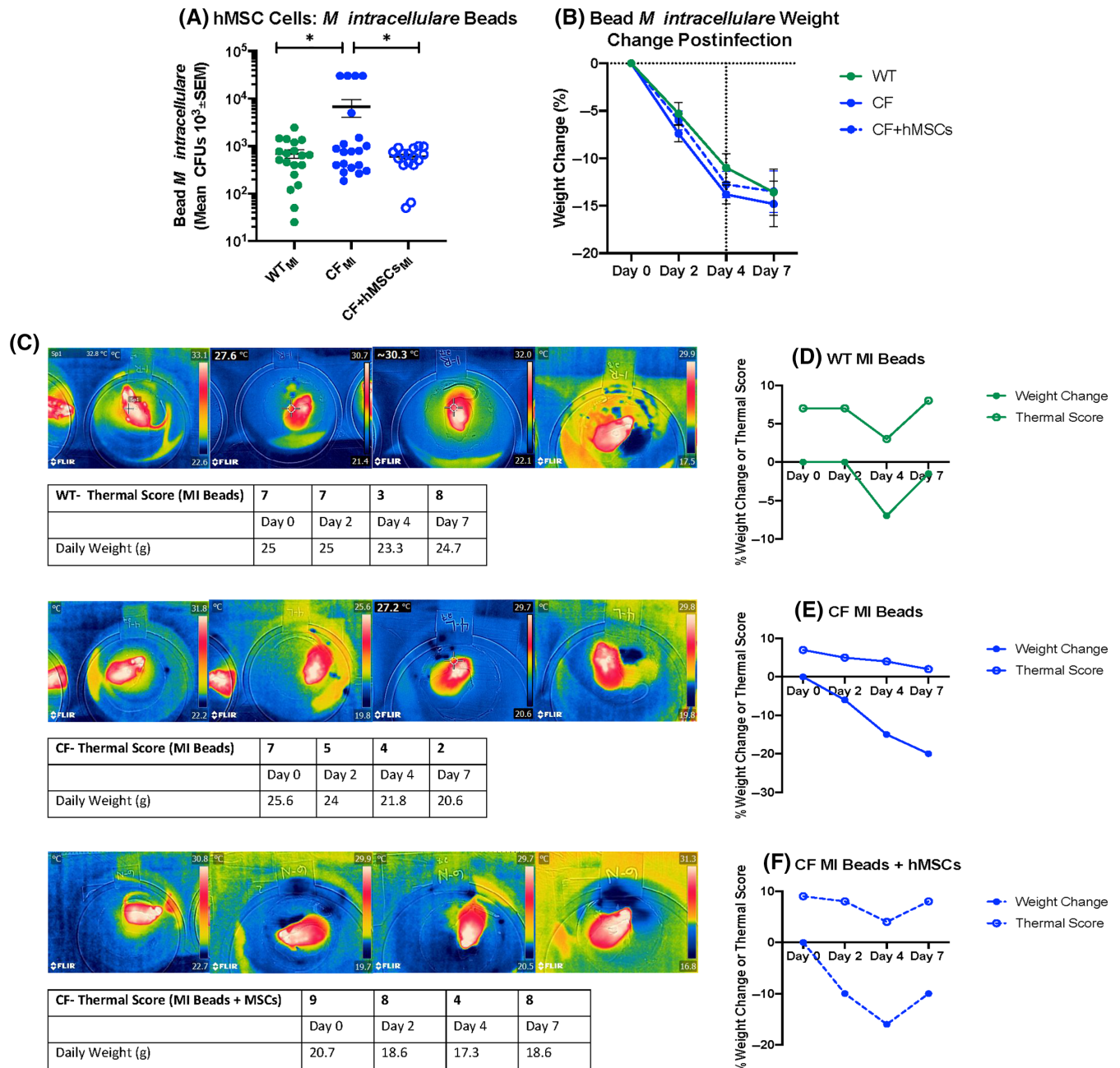


FIGURE 6 In vivo sustained *M. intracellulare* infection model treated with hMSCs. WT and CF mice were infected with *M. intracellulare* beads, and a subset of CF mice was given hMSC cells retro-orbitally. Mice were followed for 7 days for weights and thermal imaging, and postmortem CFUs were collected. A, CFUs from the WT, CF, and CF + hMSC mice were determined from whole lung homogenate. hMSCs significantly decreased *M. intracellulare* CFUs in the CF mice, but there was wide variability in this reduction (D; $P < .05$). B, Weight change was evaluated as a percent change from baseline weight prior to infection. C, Thermal imaging was performed on all mice starting the day before infection. Thermal images of representative WT (top), CF (middle), and CF + hMSC (bottom) mice, along with corresponding weights and thermal scores are shown. D-F, Thermal image scores were compared with percent weight change (for representative mouse) over the course of the study to demonstrate accuracy of thermography scoring system. None of the mice had detectable spleen or blood nontuberculous mycobacterial CFUs. * $P < .05$, CF, cystic fibrosis; CF_{MI}, CF mice infected with *M. intracellulare*; CFU, colony forming unit; CF_{MI}+hMSCs = CF mice infected with *M. intracellulare* treated with hMSCs; hMSC, human mesenchymal stem cell; MI, *M. intracellulare*; WT, wild type; WT_{MI}, wild type mice infected with *M. intracellulare*; WT_{MI}+hMSCs, wild type infected with *M. intracellulare* treated with hMSCs

TABLE 2 Bone marrow-derived macrophage response to nontuberculous *M. avium* and *M. intracellulare*

Cytokine	Unstimulated		MA free		MI free		Sterile beads		MA beads		MI beads	
	Cftr+/+	Cftr-/-	Cftr+/+	Cftr-/-	Cftr+/+	Cftr-/-	Cftr+/+	Cftr-/-	Cftr+/+	Cftr-/-	Cftr+/+	Cftr-/-
IL-6	5 ± 2	3.5 ± 0.5	115 ± 1.5	137 ± 3	432 ± 12	591 ± 11	37 ± 2.5	220 ± 58	2372 ± 188	7460 ± 488	43 ± 122	2365 ± 214
TNF α	1 ± 0.1	1 ± 0.01	379 ± 30	461 ± 22	641 ± 128	836 ± 70	371 ± 199	1412 ± 636	746 ± 58	888 ± 185	74 ± 372	836 ± 70
IL-1 β	11 ± 4	15 ± 1	109 ± 5	137 ± 3	229 ± 20	591 ± 11	74 ± 23	220 ± 58	3480 ± 648	7460 ± 488	914 ± 274	2365 ± 214
KC	120 ± 5	103 ± 2	3383 ± 14	2836 ± 208	9935 ± 152	7911 ± 255	240 ± 40	900 ± 32	4280 ± 148	2200 ± 140	3294 ± 27	2804 ± 17

Note: $P < .05$; $n = 3$. All values are pg/mL, means \pm SEM. Samples run in duplicate using Luminex Multiplex with 50 beads per cut; values were quantified after subtraction of the blank and verified for minimal nonspecific reactivity in multiplex assay.

Abbreviations: Cftr, cystic fibrosis transmembrane conductance regulator; Cftr+/+, Cftr wild type; Cftr-/-, Cftr knockout; IL, interleukin; KC, keratinocytes-derived chemokine; MA, *M. avium*; MI, *M. intracellulare*; TNF α , tumor necrosis factor α .

of the agarose bead preparations to induce BMDM cytokines, we compared the proinflammatory potency of the agarose beads embedded with *M. avium* or *M. intracellulare* with that of free *M. avium* or *M. intracellulare*, with lipopolysacchride (10ug/mL) and sterile agarose beads as positive and negative controls respectively. Table 2 shows the BMDM response to free bacteria and agarose beads embedded with bacteria.

Overall, there were pathogen-specific and cytokine-specific responses to each of the different agarose bead-NTM or free NTM conditions. The free *M. avium* and *M. intracellulare* induced a higher proinflammatory chemokine level (KC) in the CF BMDMs than the *M. avium* and *M. intracellulare* beads, which is likely due to the acute nature of the free infection. The NTM-laden beads induced higher IL-1 β expression in the CF BMDMs than in the WT, which is most likely due to the more chronic nature of the infection inducing macrophage activation. IL-6 expression was higher with the NTM-laden beads with CF BMDMs, which is consistent with CF pathophysiology and hyperproduction of IL-6 in chronic disease. TNF was elevated but not different between WT or CF in response either acute or chronic infection. In all cases, the CF BMDMs had higher levels of secreted proinflammatory cytokines in response to the NTM bead preparations than WT BMDMs (in Table 2; $P < .05$), consistent with the CF response.

3.5 | Transcriptional analysis for genes defining hMSC potency in response to NTM

We wanted to use hMSC response as a means to correlate hMSC potency and efficacy to begin to understand what might differentiate a specific hMSC preparation for potency in treating NTMs. As a follow-up to previous studies, LL-37 was quantified in the supernatant derived from the hMSCs, showing significant variability but no association with anti-NTM potency (mean \pm SD, 17192 \pm 9345 pg/mL; $n = 12$; range, 5344-32 379 pg/mL). The hMSCs that generated the supernatants screened in the antimicrobial assays presented in Figures 2 and 3 were evaluated for other biological response mediators suggested to contribute to the management of NTM infections: IL-6, HMOX-1, and CCL20 (Figure 7A-C), using gene expression profiling. TNF α was not pursued because the cytokine levels were not different between the WT and CF BMDM response to pathogens (Table 2). In these experiments, each of the different hMSC preparations was treated with either free *M. intracellulare* or *M. intracellulare* embedded onto agarose beads and followed for their gene expression profiles. When each hMSC preparation was evaluated individually (Figure 7), there was significant differences in overall response whether the *M. intracellulare* was free or embedded in the agarose beads ($P \leq .05$ comparing hMSC with pathogen vs hMSC without pathogen for each preparation individually). There was no detectable LL-37 transcriptional response (data not shown). These studies suggest that the hMSC cytokine gene expression signature may be able to define anti-NTM potency, if gene expression profiles predict therapeutic functionality.

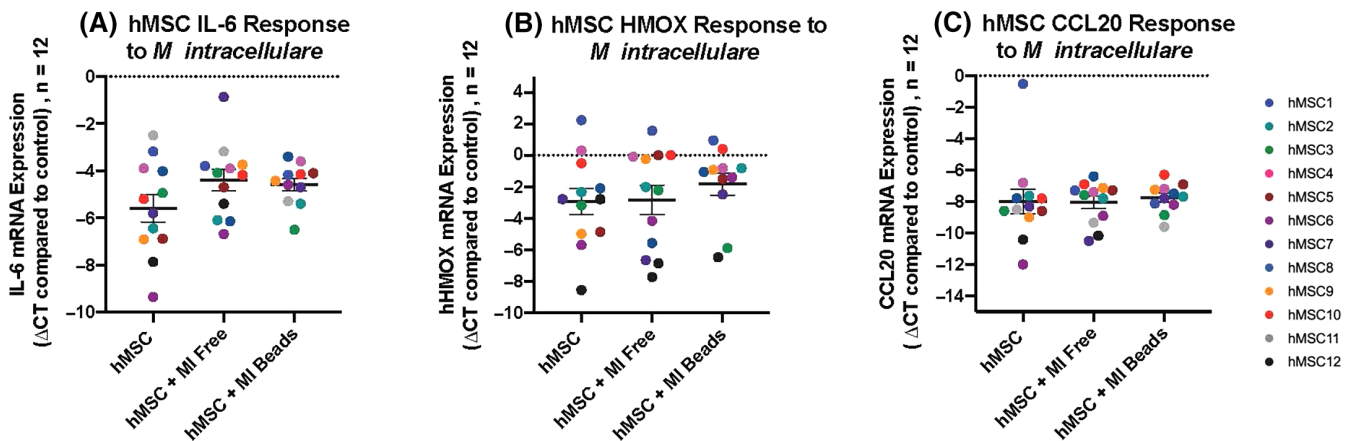


FIGURE 7 hMSC biomolecule inflammation and nontuberculous mycobacteria (NTM) infection modifiers. hMSCs from the donors profiled for anti-nontuberculous mycobacterial potency were cultured directly with *M. intracellulare* in a free slurry or embedded in agarose beads. Each of the hMSC donors was evaluated for cytokine gene expression post-mRNA/cDNA processing, focusing on biomolecules implicated in NTM management. hMSCs were screened for three main genes, IL-6 (A), hHMOX (B), and CCL20 (C). Each different preparation had a unique gene expression fingerprint for these specific proteins. The mean values were not different between the different treatment groups for each of the genes given the diversity in the hMSC fingerprint. Each individual hMSC preparation was treated with either free MI or MI embedded in agarose beads but served as its own control; the hMSC donor phenotype becomes apparent. The treatment profiles for each donor were statistically significant for individual donor responses in most cases, especially with regards to IL-6 ($P < .05$) and CCL20 ($P < .05$). Δ CT, cycle threshold; CCL20, macrophage inflammatory protein 3 α ; hHMOX, human heme oxygenase; hMSC, human mesenchymal stem cell; IL, interleukin; MI, *M. intracellulare*

4 | DISCUSSION

NTM infections can be chronic and very difficult to resolve. Based upon our previous work, we have delineated the anti-inflammatory-, antimicrobial-, and antibiotic-enhancing potential of hMSCs to aid in treating chronic nontuberculous mycobacterial infections.^{9,11,12} In our initial studies, we focused on defining the anti-NTM potency of hMSCs as well as the variability between different hMSC preparations. The results of our findings demonstrated the significant variability and potency of hMSCs against MAC (combined *M. intracellulare* and *M. avium*) as well as *M. intracellulare* and *M. avium* individually. These studies ultimately point out that not all hMSC preparations have the same level of antimicrobial potency or sustainability in activity, suggesting that it is essential to identify the appropriate hMSC donor and subsequent preparation for disease-specific applications.

To refine these criteria, we developed *in vitro* and *in vivo* models of *M. avium* and *M. intracellulare* in which we tested hMSC preparations for anti-NTM activity. In the validation of the hMSCs, we used the CF pulmonary phenotype to define disease in response to NTM infections. The CF phenotype has an increased susceptibility to the NTM infections as well as enhanced inflammatory response to pathogens. We further standardized *in vivo* models of both acute and sustained *M. intracellulare* and *M. avium* infection. The acute model did not generate a long enough infection to evaluate the hMSC potency. Using our extensive experience with developing *in vivo* modeling, agarose beads were used to sustain NTMs in the lungs to provide an *in vivo* setting for testing hMSC anti-NTM potency. The studies to directly correlate different hMSCs in both the WT and the CF models are ongoing with the ultimate goal of defining the functional variability *in vitro* with

in vivo endpoints. These studies, although they are in the early stages, are the first of their kind against NTMs.

Up to 7% of Western society suffers from a chronic inflammatory disease.⁴⁵ Rates of inflammatory conditions, including diabetes, autoimmune disorders, cardiovascular diseases, and respiratory diseases, have increased significantly in the last three decades.⁴⁶ Chronic inflammation is often concurrent with infection, increasing mortality rates among suffering individuals.^{47,48} NTMs colonize individuals with chronic lung diseases, and the treatment options for patients suffering from these diseases include immunotherapies, steroids, macrolides, and heavy antibiotic courses.⁴⁹ Many of these treatments are ineffective or have significant and long-lasting side effects such as antibiotic resistance, heart enlargement, or the development of cancer.⁵⁰⁻⁵² Patients who suffer from chronic and insidious infections with NTMs must deal not only with the consequences of the disease but also the toxicity and side effects of the long-term therapeutic intervention.^{3,50} The translation of a new therapeutic from laboratory innovation to a clinical setting requires a stepwise development and preclinical validation before use in patients. Models that mimic what happens in sustained NTM infections have been difficult to establish because small animal models clear bacteria quickly and larger animals are too expensive for defining dosing, timing, and duration of a new treatment.^{4,53} The numbers required to power these types of studies make them costly. This article demonstrates the development of an *in vivo* mouse model of sustained NTM infection, using a standardized agarose bead model and a variety of different technological approaches to validation.^{42,54} Using this modeling system, this article demonstrates a means by which NTM infections can be sustained *in vivo*. Future studies are ongoing to define a long-term model for therapeutic testing.

hMSCs are a relatively new and exciting therapeutic option for the treatment of chronic inflammation and infection given their unique capacity to respond and actively contribute to their host environment.⁵⁵ The differences between hMSCs and other pharmaceutical therapeutics lies in the “dynamic” nature of hMSC paracrine repertoires responsible for clinical effectiveness.⁵⁶ Many subjects enrolled in clinical trials involving hMSC therapeutics experience dramatic clinical success; however, there is a significant nonresponder population that does not obtain benefits from the same therapy.⁵⁷ The effectiveness of hMSC therapeutic contributions is dictated by disease severity and the hMSC phenotype contributing to an inefficient hMSC therapeutic. The validation of “bench-to-bedside” modeling systems to mimic chronic NTM is essential to identify the best culturing conditions that result in optimal and reproducible assays for hMSC clinical potency for the disease-specific pathophysiology for treating diseases such as NTM lung infections.

hMSCs have the potential of managing infection and inflammation through both direct and indirect interactions with the host. The production of soluble antibacterial mediators like LL-37 and CCL20 directly support immune cell recruitment and antimicrobial activity.^{11,58-60} These antimicrobial peptides can define the phenotype of the initial host response to infection as well as directly interact with the pathogen, increasing susceptibility to antibiotics and other pharmaceuticals aimed at slowing or killing the bacteria directly. Our studies here did not find correlation between the production of LL-37 and anti-NTM activity. LL-37 is highly complex with the capacity to drill pores into extracellular pathogens and provide a chemotactic gradient for cellular recruitment.^{11,61} NTMs are intracellular pathogens, using macrophages to optimize pathogenicity and potentially protecting themselves from host antimicrobial activity.^{4,62} LL-37 may be very important in providing efficiency in immune clearance of NTMs but may not have a direct impact on pathogen survival.^{62,63} This represents collaborative work ongoing in our laboratory. To follow up on these studies, we focused on monitoring soluble factors that have been directly linked to NTM management in the literature.^{64,65} hMSC mediators, such as HMOX-1, indoleamine-pyrrole 2,3-dioxygenase (IDO), IL-17, IL-6, IL-8, and IL-10, can redirect host immunity by affecting macrophage and T-cell phenotypes for specific adaptive and innate mechanism to support the host in the pursuit of homeostasis.⁶⁶⁻⁶⁹ Depending on the host milieu and the unique phenotype of the hMSC donor, it is easy to understand the variability in host responsiveness to cell-based hMSC therapy. Every donor hMSC preparation has a unique profile in terms of response to pathogens, which likely translates into the downstream events related to successful potency and host response to treatment. Future studies are planned to evaluate unique hMSC fingerprints associated with antimicrobial potency and whether it is global or pathogen specific.

5 | CONCLUSION

Sustained infection and inflammation are often associated with infection with bacteria such as NTM species *M. avium* and *M.*

intracellulare.⁴⁶ hMSCs are therapeutic tools that have been studied in more than 1200 clinical trials associated with some aspect of inflammation and infection (ClinicalTrials.gov). hMSCs are unique in their capacity to respond by secreting multiple bioactive factors and actively contributing to the host environment; this gives the hMSCs a clinical advantage over traditional pharmaceuticals.^{34,70} In this article, a strategy has been developed focusing on selecting an hMSC product that had the highest in vitro and in vivo preclinical potency against *M. intracellulare* and *M. avium*. Furthermore, through effector modification of hMSCs and clinically translational modeling systems, the studies in this article will be able to bridge the gap between bench validation and clinical implementation of the “ideal” hMSC donor and resultant phenotype for the treatment of pulmonary diseases complicated with NTM mycobacterial infections.

ACKNOWLEDGMENTS

We thank Lauren Auster, Mary Chandler-Gwin, Kelly Sopko, Karen Folz, Zachary Hostoffer, and Margie Harris for their technical assistance; Alma Wilson, Brittany Burns, and Molly Schneider of the CF Animal Core under the direction of Craig Hodges; and the Clinical and Translational Science Collaborative (CTSC) Bioanalyte Core, directed by Dr Bonfield. This study was supported by The Marcus Foundation, the Cystic Fibrosis Foundation, and the David and Virginia Baldwin Fund.

CONFLICT OF INTEREST

The authors declared no potential conflicts of interest.

AUTHOR CONTRIBUTIONS

T.L.B.: conception/design, financial support, collection and/or assembly of data, data analysis and interpretation, manuscript writing, final approval of manuscript; M.S., M.F.: collection and/or assembly of data, data analysis and interpretation, manuscript writing; D.F.: collection and/or assembly of data, data analysis and interpretation; V.R.: collection and/or assembly of data, manuscript writing; R.A.S.: provision of study material or patients; A.I.C.: conception/design, financial support, provision of study material or patients, data analysis and interpretation, manuscript writing, final approval of manuscript.

DATA AVAILABILITY STATEMENT

All data are available for review from the corresponding author and Case Western Reserve University.

ORCID

Tracey L. Bonfield  <https://orcid.org/0000-0001-9698-9113>

Rodrigo A. Somoza  <https://orcid.org/0000-0001-8050-357X>

Arnold I. Caplan  <https://orcid.org/0000-0002-8677-6621>

REFERENCES

1. Drummond WK, Kasperbauer SH. Nontuberculous mycobacteria: epidemiology and the impact on pulmonary and cardiac disease. *Thorac Surg Clin*. 2019;29:59-64.
2. Honda JR, Alper S, Bai X, Chan ED. Acquired and genetic host susceptibility factors and microbial pathogenic factors that predispose to

- nontuberculous mycobacterial infections. *Curr Opin Immunol*. 2018; 54:66-73.
3. Lakoš AK, Pangerčič A, Gašparič M, et al. Safety and effectiveness of azithromycin in the treatment of respiratory infections in children. *Curr Med Res Opin*. 2012;28:155-162.
 4. Swenson C, Zerbe CS, Fennelly K. Host variability in NTM disease: implications for research needs. *Front Microbiol*. 2018;9:2901.
 5. Martiniano SL, Nick JA, Daley CL. Nontuberculous mycobacterial infections in cystic fibrosis. *Thorac Surg Clin*. 2019;29:95-108.
 6. Bernut A, Herrmann JL, Ordway D, et al. The diverse cellular and animal models to decipher the physiopathological traits of *Mycobacterium abscessus* infection. *Front Cell Infect Microbiol*. 2017;7:100.
 7. Auster L, Sutton MT, Gwin MC, Nitkin C, Bonfield TL. Optimization of in vitro *Mycobacterium avium* and *Mycobacterium intracellulare* growth assays for therapeutic development. *Microorganisms*. 2019;7:42-60.
 8. Caplan AI. Why are MSCs therapeutic? New data: new insight. *J Pathol*. 2009;217:318-324.
 9. Sutton MT, Fletcher D, Episalla N, et al. Mesenchymal stem cell soluble mediators and cystic fibrosis. *J Stem Cell Res Ther*. 2017;7:400.
 10. Goldstein BD, Lauer ME, Caplan AI, Bonfield TL. Chronic asthma and mesenchymal stem cells: hyaluronan and airway remodeling. *J Inflamm*. 2017;14:18.
 11. Sutton MT, Fletcher D, Ghosh SK, et al. Antimicrobial properties of mesenchymal stem cells: therapeutic potential for cystic fibrosis infection, and treatment. *Stem Cells Int*. 2016;2016:5303048.
 12. Bonfield T, Lennon D, Ghosh S, et al. Cell based therapy aids in infection and inflammation resolution in the murine model of cystic fibrosis lung disease. *Stem Cell Discov*. 2013;3:139-153.
 13. Singh N, Ahmad Z, Baid N, Kumar A. Host heme oxygenase-1: friend or foe in tackling pathogens? *IUBMB Life*. 2018;70:869-880.
 14. Vulcano M, Struyf S, Scapini P, et al. Unique regulation of CCL18 production by maturing dendritic cells. *J Immunol*. 2003;170:3843-3849.
 15. Regev D, Surolija R, Karki S, et al. Heme oxygenase-1 promotes granuloma development and protects against dissemination of mycobacteria. *Lab Invest*. 2012;92:1541-1552.
 16. Heeckeren A, Walenga R, Konstan MW, Bonfield T, Davis PB, Ferkol T. Excessive inflammatory response of cystic fibrosis mice to bronchopulmonary infection with *Pseudomonas aeruginosa*. *J Clin Invest*. 1997;100:2810-2815.
 17. Hsu D, Taylor P, Fletcher D, et al. Interleukin-17 pathophysiology and therapeutic intervention in cystic fibrosis lung infection and inflammation. *Infect Immun*. 2016;84:2410-2421.
 18. Bruscia EM, Zhang PX, Barone C, et al. Increased susceptibility of Cfr^{-/-} mice to LPS-induced lung remodeling. *Am J Physiol Cell Mol Physiol*. 2016;310:L711-L719.
 19. Soltys J, Bonfield TL, Chmiel J, Berger M. Functional IL-10 deficiency in the lung of cystic fibrosis (cfr^{-/-}) and IL-10 knockout mice causes increased expression and function of B7 costimulatory molecules on alveolar macrophages. *J Immunol*. 2002;168:1903-1910.
 20. Bragonzi A. Murine models of acute and chronic lung infection with cystic fibrosis pathogens. *Int J Med Microbiol*. 2010;300:584-593.
 21. Hodges CA, Cotton CU, Palmert MR, Drumm ML. Generation of a conditional null allele for Cfr in mice. *Genesis*. 2008;46:546-552.
 22. Semaniakou A, Croll RP, Chappe V. Animal models in the pathophysiology of cystic fibrosis. *Front Pharmacol*. 2019;9:1475.
 23. Bonfield TL. Preclinical modeling for therapeutic development in cystic fibrosis. *Am J Respir Crit Care Med*. 2020;201:267-268.
 24. Babaev VR, Yancey PG, Ryzhov SV, et al. Conditional knockout of macrophage PPAR γ increases atherosclerosis in C57BL/6 and low-density lipoprotein receptor-deficient mice. *Arterioscler Thromb Vasc Biol*. 2005;25:1647-1653.
 25. Bonfield TL, Swaisgood CM, Barna BP, Farver CF, Kavuru MS, Thomassen MJ. Elevated gelatinase activity in pulmonary alveolar proteinosis: role of macrophage-colony stimulating factor. *J Leukoc Biol*. 2006;79:133-139.
 26. Chmiel JF, Konstan MW, Knesebeck JE, et al. IL-10 attenuates excessive inflammation in chronic *Pseudomonas* infection in mice. *Am J Respir Crit Care Med*. 1999;160:2040-2047.
 27. Paroni M, Moalli F, Nebuloni M, et al. Response of CFTR-deficient mice to long-term chronic *Pseudomonas aeruginosa* infection and PTX3 therapy. *J Infect Dis*. 2013;208:130-138.
 28. Wilke M, Buijs-Offerman RM, Aarbiou J, et al. Mouse models of cystic fibrosis: phenotypic analysis and research applications. *J Cyst Fibros*. 2011;10(suppl 2):S152-S171.
 29. van Heeckeren AM, Schluchter MD, Xue W, Davis PB. Response to acute lung infection with mucoid *Pseudomonas aeruginosa* in cystic fibrosis mice. *Am J Respir Crit Care Med*. 2006;173:288-296.
 30. van Heeckeren AM, Schluchter MD. Murine models of chronic *Pseudomonas aeruginosa* lung infection. *Lab Anim*. 2002;36:291-312.
 31. van Heeckeren AM, Tscheikuna J, Walenga RW, et al. Effect of *Pseudomonas* infection on weight loss, lung mechanics, and cytokines in mice. *Am J Respir Crit Care Med*. 2000;161:271-279.
 32. Lennon DP, Caplan AI. Isolation of human marrow-derived mesenchymal stem cells. *Exp Hematol*. 2006;34:1604-1605.
 33. Lin P, Lin Y, Lennon DP, Correa D, Schluchter M, Caplan AI. Efficient lentiviral transduction of human mesenchymal stem cells that preserves proliferation and differentiation capabilities. *STEM CELLS TRANSLATIONAL MEDICINE*. 2012;1:886-897.
 34. Bonfield TL, Nolan Koloze MT, Lennon DP, et al. Defining human mesenchymal stem cell efficacy in vivo. *J Inflamm*. 2010;7:51.
 35. Czaplaj J, Matuszczak S, Kulik K, et al. The effect of culture media on large-scale expansion and characteristic of adipose tissue-derived mesenchymal stromal cells. *Stem Cell Res Ther*. 2019;10:235.
 36. Bonfield TL, John N, Barna BP, Kavuru MS, Thomassen MJ, Yen-Lieberman B. Multiplexed particle-based anti-granulocyte macrophage colony stimulating factor (GM-CSF) assay: a pulmonary diagnostic test. *Clin Diagn Lab Immunol*. 2005;12:821-824.
 37. Nitkin CR, Bonfield TL. Balancing anti-inflammatory and anti-oxidant responses in murine bone marrow derived macrophages. *PLoS One*. 2017;12:e0184469.
 38. Peppers BP, Vatsayan A, Dalal J, Bonfield T, Tcheurekdjian H, Hostoffer R. A case series: association of anaphylaxis with a significant decrease in platelet levels and possible secondary risk of thrombosis. *Immun Inflamm Dis*. 2018;6:377-381.
 39. Ogura T, Yanagimoto T. Improving and extending the McNemar test using the Bayesian method. *Stat Med*. 2016;35(14):2455-2466. <https://doi.org/10.1002/sim.6875>
 40. Simon R, Radmacher MD, Dobbin K. Design of studies using DNA microarrays. *Genet Epidemiol*. 2002;23:21-36.
 41. Klemens SP, Cynamon MH, Swenson CE, Ginsberg RS. Liposome-encapsulated-gentamicin therapy of *Mycobacterium avium* complex infection in beige mice. *Antimicrob Agents Chemother*. 1990;34:967-970.
 42. Peppers BP, Jhaveri D, Van Heeckeren R, et al. Stratification of peanut allergic murine model into anaphylaxis severity risk groups using thermography. *J Immunol Methods*. 2018;459:29-34.
 43. Bruscia EM, Zhang PX, Ferreira E, et al. Macrophages directly contribute to the exaggerated inflammatory response in cystic fibrosis transmembrane conductance regulator^{-/-} mice. *Am J Respir Cell Mol Biol*. 2009;40:295-304.
 44. Bonfield TL, Hodges CA, Cotton CU, Drumm ML. Absence of the cystic fibrosis transmembrane regulator (Cfr) from myeloid-derived cells slows resolution of inflammation and infection. *J Leukoc Biol*. 2012; 92:1111-1122.
 45. Walsh GM. Targeting airway inflammation: novel therapies for the treatment of asthma. *Curr Med Chem*. 2006;13:3105-3111.
 46. Inamdar AC, Inamdar AA. Mesenchymal stem cell therapy in lung disorders: pathogenesis of lung diseases and mechanism of action of mesenchymal stem cell. *Exp Lung Res*. 2013;39:315-327.

47. Bezzeri V, Piacenza F, Caporelli N, Malavolta M, Provinciali M, Cipolli M. Is cellular senescence involved in cystic fibrosis? *Respir Res*. 2019;20:32-44.
48. Boyton RJ, Altmann DM. Bronchiectasis: current concepts in pathogenesis, immunology, and microbiology. *Annu Rev Pathol*. 2016;11:523-554.
49. Belvisi MG, Hele DJ, Birrell MA. New advances and potential therapies for the treatment of asthma. *BioDrugs*. 2004;18:211-223.
50. Velicer CM, Heckbert SR, Lampe JW, Potter JD, Robertson CA, Taplin SH. Antibiotic use in relation to the risk of breast cancer. *JAMA*. 2004;291:827-835.
51. Kwon YS, Koh WJ, Daley CL. Treatment of *Mycobacterium avium* complex pulmonary disease. *Tuberc Respir Dis*. 2019;82:15-26.
52. Cowman S, Burns K, Benson S, Wilson R, Loebinger MR. The antimicrobial susceptibility of non-tuberculous mycobacteria. *J Infect*. 2016;72:324-331.
53. Falkinham JO III. Challenges of NTM drug development. *Front Microbiol*. 2018;9:1613.
54. Soltzberg J, Frischmann S, van Heeckeren C, Brown N, Caplan A, Bonfield TL. Quantitative microscopy in murine models of lung inflammation. *Anal Quant Cytol Histol*. 2011;33:245-252.
55. Tyndall A, Walker UA, Cope A, et al. Immunomodulatory properties of mesenchymal stem cells: a review based on an interdisciplinary meeting held at the Kennedy Institute of Rheumatology Division, London, UK, October 31, 2005. *Arthritis Res Ther*. 2007;9:301.
56. Caplan AI, Dennis JE. Mesenchymal stem cells as trophic mediators. *J Cell Biochem*. 2006;98:1076-1084.
57. Caplan AI. Cell-based therapies: the nonresponder. *STEM CELLS TRANSLATIONAL MEDICINE*. 2018;7:762-766.
58. Krasnodembskaya A, Song Y, Fang X, et al. Antibacterial effect of human mesenchymal stem cells is mediated in part from secretion of the antimicrobial peptide LL-37. *STEM CELLS*. 2010;28:2229-2238.
59. Yasir M, Dutta D, Willcox MDP. Comparative mode of action of the antimicrobial peptide melimine and its derivative Mel4 against *Pseudomonas aeruginosa*. *Sci Rep*. 2019;9:7063.
60. Weiskopf D, Weinberger B, Grubeck-Loebenstein B. The aging of the immune system. *Transpl Int*. 2009;22:1041-1050.
61. Weinberg A, Jin G, Sieg S, et al. The yin and yang of human beta-defensins in health and disease. *Front Immunol*. 2012;3:294.
62. Kim SY, Chang B, Jeong BH, et al. Implication of vitamin D-associated factors in patients with nontuberculous mycobacterial lung disease. *Int J Tuberc Lung Dis*. 2016;20:1594-1602.
63. Yang B, Good D, Mosaib T, et al. Significance of LL-37 on immunomodulation and disease outcome. *Biomed Res Int*. 2020;2020:8349712.
64. Suroliá R, Karki S, Wang Z, et al. Attenuated heme oxygenase-1 responses predispose the elderly to pulmonary nontuberculous mycobacterial infections. *Am J Physiol Lung Cell Mol Physiol*. 2016;311:L928-L940.
65. Awuh JA, Flo TH. Molecular basis of mycobacterial survival in macrophages. *Cell Mol Life Sci*. 2017;74:1625-1648.
66. Murphy MB, Moncivais K, Caplan AI. Mesenchymal stem cells: environmentally responsive therapeutics for regenerative medicine. *Exp Mol Med*. 2013;45:e54.
67. Naito Y, Takagi T, Higashimura Y. Heme oxygenase-1 and anti-inflammatory M2 macrophages. *Arch Biochem Biophys*. 2014;564:83-88.
68. Caplan AI. Mesenchymal stem cells: time to change the name! *STEM CELLS TRANSLATIONAL MEDICINE*. 2017;6:1445-1451.
69. Saldaña L, Bensiamar F, Vallés G, Mancebo FJ, García-Rey E, Vilaboia N. Immunoregulatory potential of mesenchymal stem cells following activation by macrophage-derived soluble factors. *Stem Cell Res Ther*. 2019;10:58.
70. Caplan AI, Correa D. The MSC: an injury drugstore. *Cell Stem Cell*. 2011;9:11-15.

How to cite this article: Bonfield TL, Sutton MT, Fletcher DR, et al. Donor-defined mesenchymal stem cell antimicrobial potency against nontuberculous mycobacterium. *STEM CELLS Transl Med*. 2021;10:1202-1216. <https://doi.org/10.1002/sctm.20-0521>